OFFICE OF NAVAL RESEARCH

GRANT or CONTRACT: N00014-91-J-1919

96PRO-2855
Robert Nowak

Technical Report No. 25

Se Addlattices formed on Au(100), Studies by LEED, AES, STM and Electrochemistry

Baoming M. Huang, Tedd E. Lister and John L. Stickney

Submitted to

Surface Science

Department of Chemistry
University of Georgia
Athens, GA 30602-2556

10/15/96

DISCLAIMER NOTICE

THIS DOCUMENT IS BEST QUALITY AVAILABLE. THE COPY FURNISHED TO DTIC CONTAINED A SIGNIFICANT NUMBER OF PAGES WHICH DO NOT REPRODUCE LEGIBLY.

REPORT DOCUMENTATION PAGE

Form Approved
OMB No. 0704-0188

1. AGENCY USE ONLY (Leave blank)	2. REPORT DATE	3. REPORT TYPE AND DATES COVERED
	10/15/96	Technical 6/1/95 - 10/15/96

4. TITLE AND SUBTITLE
Se Addlattices Formed on Au(100), Studies by LEED, AES, STM and Electrochemistry

5. FUNDING NUMBERS
G-N00014-19-J-1919
Dr. Robert J. Nowak
96PRO-2855

6. AUTHOR(S)
Baoming M. Huang, Tedd E. Lister and John L. Stickney

7. PERFORMING ORGANIZATION NAME(S) AND ADDRESS(ES)
John L. Stickney
Department of Chemistry
University of Georgia
Athens, GA 30602-2556

8. PERFORMING ORGANIZATION REPORT NUMBER
Technical Report #25

9. SPONSORING / MONITORING AGENCY NAME(S) AND ADDRESS(ES)
Office of Naval Research
Chemistry Division
800 North Quincy Street
Arlington, VA 22217-5660

10. SPONSORING / MONITORING AGENCY REPORT NUMBER

11. SUPPLEMENTARY NOTES

12a. DISTRIBUTION / AVAILABILITY STATEMENT
Approved for public release and sale; its distribution is unlimited

12b. DISTRIBUTION CODE

13. ABSTRACT *(Maximum 200 words)*

Ordered selenium atomic layers have been formed electrochemically on Au(100) at a series of coverages. Cyclic voltammetry and coulometry were used to study the deposition process, and to determine the corresponding coverages of a number of Se structures. Structures, with Se coverages of 1/4, 1/3, ½, and 8/9 monolayers (ML), were identified using ultra high vacuum - electrochemical (UHV-EC) techniques as well as scanning tunneling microscopy (STM). The corresponding unit cells of those structures were: p(2X2), (2X 10), c(2X2), and mostly (3X 10), composed of close-packed Se_8 rings. Pit formation, associated with formation of the densely packed Se_8 ring structure, was observed, and is reminiscent of pits observed in self assembly monolayers (SAMs) of alkane thiols on Au surfaces. The pits disappeared as the structure composed of Se rings, was converted to lower coverage structures, such as the 1/4 ML p(2X2), via anodic stripping. Se atomic layers were formed electro- chemically in three ways: direct reduction from a $HSeO_3^-$ solution, anodic stripping of previously formed bulk Se, or cathodic stripping of previously formed bulk Se. All three methods resulted in equivalent atomic layer structures on the Au(100) surface, but with some variation in the homogeneity and distribution of particular structures.

14. SUBJECT TERMS	15. NUMBER OF PAGES
Electrodeposition, Se, UPD, LEED, STM, AES, Au(100)	44
	16. PRICE CODE

17. SECURITY CLASSIFICATION OF REPORT	18. SECURITY CLASSIFICATION OF THIS PAGE	19. SECURITY CLASSIFICATION OF ABSTRACT	20. LIMITATION OF ABSTRACT
Unclassified	Unclassified	Unclassified	UL

Submitted to Surface Science, 7/25/96

Se ADDLATTICES FORMED ON Au(100), STUDIES BY LEED, AES, STM AND ELECTROCHEMISTRY

Baoming M. Huang, Tedd E. Lister and John L. Stickney*

Department of Chemistry, The University of Georgia, Athens, GA 30602-2556

Tel: (706) 542-1967

FAX: (706) 542-9454

E-mail: stickney@sunchem.chem.uga.edu

* To whom correspondence should be addressed.

ABSTRACT

Ordered selenium atomic layers have been formed electrochemically on Au(100) at a series of coverages. Cyclic voltammetry and coulometry were used to study the deposition process, and to determine the corresponding coverages of a number of Se structures. Structures, with Se coverages of 1/4, 1/3, 1/2, and 8/9 monolayers (ML), were identified using ultra high vacuum - electrochemical (UHV-EC) techniques as well as scanning tunneling microscopy (STM). The corresponding unit cells of those structures were: p(2X2), ($2X\sqrt{10}$), c(2X2), and a mostly ($3X\sqrt{10}$), composed of close-packed Se_8 rings. Pit formation, associated with formation of the densely packed Se_8 ring structure, was observed, and is reminiscent of pits observed in self assembly monolayers (SAMs) of alkane thiols on Au surfaces. The pits disappeared as the structure composed of Se rings, was converted to lower coverage structures, such as the 1/4 ML p(2X2), via anodic stripping. Se atomic layers were formed electrochemically in three ways: direct reduction from a $HSeO_3^-$ solution, anodic stripping of previously formed bulk Se, or cathodic stripping of previously formed bulk Se. All three methods resulted in equivalent atomic layer structures on the Au(100) surface, but with some variation in the homogeneity and distribution of particular structures.

INTRODUCTION

Atomic layer epitaxy (ALE) is a method of forming thin films of materials an atomic layer at a time, using surface limited reactions to control the growth rate and morphology [1-3]. For compounds, a cycle is used to grow individual monolayers of the compound. The electrochemical analog of ALE is presently being developed in this group [4-8]. Electrochemical ALE (ECALE) makes use of underpotential deposition (UPD), which is another way of describing a surface limited electrodeposit [9-11]. A cycle in the ECALE deposition of a compound, then, involves the alternated UPD of atomic layers of the individual elements.

Studies of the surface limited electrodeposition of atomic layers, of the individual elements making up II-VI compounds, have been a major thurst of work in this group [12-19]. Ultra high vacuum surface analysis techniques combined directly with electrochemical cells (UHV-EC), and scanning tunneling microscopy (STM), have been used to study the structures of atomic layers of the constituent elements and compound monolayers on single crystal electrodes [12-15]. As well, thin layer electrodes (TLEs) and cyclic voltammetry have been used to study the optimum potentials and solution compositions, needed to develop ECALE cycles, for a number of compounds [16,17]. In addition, an automated flow-cell deposition system has been developed, and used to form thin films by the ECALE methodology [18,19].

The present study concerns the growth of the first atomic layer of selenium on a Au(100) single crystal substrate, as the first step in the ECALE formation of selenium based compounds, such as CdSe, ZnSe or $CuInSe_2$. From a more fundamental point of view, this work is also the first study of the surface structures formed during the UPD of Se.

Electrodeposition of Se on Au has been studied previously by several workers [20-22]. Those studies, however, focused on either the reduction pathway for $HSeO_3^-$ [20], the deposition of bulk Se [21], or the analysis of trace amount of Se [22]. The surface structures formed by monolayer amount of Se on Au have not been reported. STM has been used by one group to study the structures of Se atomic layers on graphite surfaces [23]. Those authors claim that Se_6 rings were formed, but no atomically resolved images were reported.

The surface structures of Te and S have been the subjects of several papers [13,24-28]. A number of interesting surface chalcogenide species were formed, including: chains of dimers in the case of Te, and 8 membered rings in the case of S. In studies of self assembly monolayers of alkane thiols on Au, 8 membered rings were also observed [29-35].

Formation of CdTe monolayers, by the electrodeposition of Cd on Te atomic layers, has been studied on the low index planes of Au. The CdTe monolayer on Au(100) resembled a CdTe(100) planes cut out of the bulk zinc blend structure of CdTe, with a 10% compression of the CdTe lattice in order to match up with the substrate [13]. The structure of the CdTe monolayer deposited on Au(100), involved a c(2X2) unit cell, and 1/2 coverages of both Te and Cd. The lattice match for CdSe with Au(100) should be more favorable, 3% (0.605 nm for CdSe vs. 0.584 nm for twice the Au-Au distance) [7]. A Se coverage of 1/2, for the first atomic layer, is then expected to be optimum for the growth of CdSe using jthe ECALE methodology.

EXPERIMENTAL

Two Au(100) single crystals were used in this study. One of them was a six-sided Au(100), with all six faces oriented and polished to {100}. The other was a Au(100) disc, 1 cm in diameter and 2 mm thick, the top and bottom faces of which were oriented and polished to {100}. The six-sided crystal was used for voltammetry, coulometry, and UHV-EC studies, while the Au(100) disc was used for STM imaging. Both crystals were oriented using Laue back scattering X-ray diffraction, and polished using a two axis goniometer. The crystal surfaces were then electropolished, cleaned in hot concentrated nitric acid, and flamed annealed in a gas-oxygen torch prior to use. In most cases, the crystals were electrochemically annealed with iodide by immersion at -100 mV (vs. Ag/AgCl, 1 M NaCl) in a solution containing 5 mM KI + 20 mM H_2SO_4, for 2 minutes prior to the experiments, in order to atomically level the Au surfaces [36].

The geometric surface area of the six-sided Au(100) was 1.8 ± 0.1 cm^2. The method of Soriaga and co-workers was also used to determine the active surface area of the crystal, using adsorbed iodine [37], and yielded a surface area of 1.88 ± 0.08 cm^2, which was used in coverage calculations.

Solutions were prepared with Puratronic grade SeO_2 (Johnson Matthey); analytical grade H_2SO_4, acetic acid, sodium acetate, and borate; and 18 M ohm-cm water obtained from a Barnstead Nano-pure filtration system, fed from the house distilled water supply. All solutions were deoxygenated with N_2 gas, prior to the start of each experiment. Cyclic voltammetry studies were carried out in a conventional two-compartment H-cell, with an op-amp based potentiostat, built in house. The reference electrode was a Ag/AgCl (1.0 M NaCl) electrode, to which all potentials have been referenced. A gold wire was used as the auxiliary electrode.

STM studies were performed with a Nanoscope III, Digital Instruments. The surface structures of Se atomic layers on Au(100) were imaged either in air or *in situ* (in solution, under potential control). The tips were prepared by electrochemical etching of W wires in 1 M KOH. Nail polish (Wet' n' Wild, Pavion) was used to coat the tips, and prevent excess Faradaic currents for *in-situ* imaging.

RESULTS AND DISCUSSION

Voltammetry

Figure 1 is the cyclic voltammogram of the clean six-sided Au(100) electrode in a 20 mM H_2SO_4 solution. The main feature is the oxidation of the Au surface to form a monolayer of surface oxide/hydroxide at potentials above 900 mV, while reversal of the scan direction at 1.2 V resulted in its reduction. Between 900 mV and -350 mV, the only charge observed is that associated with the electrochemical double layer. At -350 mV, hydrogen evolution was initiated.

Figure 2 is for the same electrode immersed in a solution containing 1 mM $HSeO_3^-$ and 20 mM H_2SO_4. A sequence of cyclic voltammograms were run, each to a successively lower potential, in a "window opening" experiment. The sequential scans are presented alternately as solid and dashed lines. At least five reduction features are evident in the negative going scans, A-E, while there are three oxidative stripping features, A'-C'.

The charge in the first reduction peak, A, is indicative of a UPD process. That is, the corresponding coverage is 1/3 monolayer (ML), relative to the number of Au surface atoms. The shoulder, B, is small and accounts for an increase in coverage of only about 1/6 ML. This charge could be due to deposition at defects sites and polycrystalline parts of the electrode, or to a phase

change, such as that which would accompany the formation of a second structure at a slightly higher coverage. The formal potential appears to be about 400 mV, positive of even peak A, which indicates that peaks A and B are in fact deposition at an overpotential, indicating slow deposition kinetics. Temperature dependent studies, however, indicate little shift in peak potentials, even at 80 °C. Peak C corresponds to the deposition of about 1.5 ML of Se, considerably more than expected for a UPD process, especially since 1/2 ML has already been deposited in peaks A and B. Most UPD involves the formation of a single atomic layer [9-11]. There are, however, some systems where a second layer is formed at underpotential as well, such as Tl [38]. There are also cases where the presence of a pre-adsorbed layer of a third element can result in UPD of more than a single ML: Ag UPD on Pt(111)($\sqrt{7}$ X $\sqrt{7}$)R19.1°-I [39], and Cu on Se coated Au [40], for instance. However, in the present case, the potential, the amounts of Se and the absence of a third element suggest that peak C is not related to a UPD process. At present, it appears that the drop in deposition current associated with peak C is the result of a change in the deposition kinetics. As mentioned above, both peaks A and B are over potential peaks, indicating slow kinetics, but the overpotential associated with peak C is still greater. Apparently, after two monolayers of Se have been deposited there is a change in the deposition mechanism, resulting in an increase in the difficulty of depositing Se.

The nature of peak D appears similar to that of C, although D does shifts to positively as the temperature is increased where as C does not. As D shifts, at higher temperatures, it combines with C. Feature E is the onset of mass transfer limited bulk Se deposition, possibly combined with some hydrogen evolution.

In the oxidative stripping scan (Figure 2), peak A' is the corresponding stripping peak for A, while B' appears to correspond to stripping of the Se deposited in B. When deposits are

formed with more Se than that contained in features A and B, the stripping feature C' appears. If peaks C and D were each the result of UPD processes, stripping the corresponding Se should show some increased stability. Separate stripping features might be expected, relative to a bulk stripping feature, and none is observed. Instead, the more Se deposited, the larger peak C' becomes, and the more positive it shifts in potential. The stripping appears to start near the formal potential, indicating that stripping is less kinetically hindered then deposition, but the thicker the initial deposit, more sluggish the kinetics become. Alternatively, the shift in potential of C' may be related to the very high resistivity of Se.

The study shown in Figure 3 was performed to investigate the kinetics responsible for the voltammetry in Figure 2. Each point in Figure 3 was obtained by scanning to the indicated potential and holding for the indicated periods of time. Anodic stripping was used to determine the resulting Se coverages. The graphs show three basic types of behavior. The deposits formed at 357, 305, and 112 mV, appear to level off over five minutes, at coverages of 1/3, 1/2, and 2 ML, respectively. The deposits formed at 225 and -150 mV both start off with higher rates of deposition, then taper off, but still have appreciable rates after 5 minutes. Lastly, the deposit formed at -350 mV has essentially a constant rate of deposition over the whole 5 minutes. For each data point in the graph, the integrated cathodic deposition charge was found to equal that of the corresponding anodic stripping charge.

These results are in general agreement with the window opening experiment (Figure 2). That is, the deposits formed at 357 and 305 mV result in the same coverages obtained from UPD peaks A and B (Figure 2). The deposit formed at 112 mV resulted in the deposition of 2 ML, corresponding closely with peak C. The deposits formed at 225 mV provide some idea of the

importance of kinetics in the formation of these deposits. Initially, after scanning to 225 mV, a 1/2 ML of Se had been deposited, while after 5 minutes at the same potential, deposition was still proceeding, and over 1 ML had been deposited, indicating that all the Se deposited in peak C was probably stable at 225 mV, but was very slow to deposit.

The deposit formed at -150 mV started out at a coverage of nearly 2.5 ML, and after 5 minutes, Se was still depositing, producing a coverage of 4 ML, again displaying the sluggishness of the process. The last potential, -350 mV, resulted in steady Se deposition, in line with mass transfer limited deposition, aided by a small amount of convection.

Se Atomic Layer Formation

Atomic layers of Se were formed electrochemically by three different methods, each resulted in essentially the same Se structures, but with some variation in the deposit homogeneity. The first involved reductive deposition of Se from a $HSeO_3^-$ solution, in experiments analogous to those shown in Figures 2 and 3. The second two methods involved the initial formation of a about 1 1/4 ML of Se and then stripping the excess at controlled potential. A graph of the coverage left after anodic stripping at a series of potentials is shown in Figure 4. The Se coverage resulting after a stripping experiment was determined coulometrically by oxidatively stripping the remaining Se. As stated above, each point in Figure 4 involved the initial deposition of 1.25 ML, thus the 1.25 ML plateau at potentials below 500 mV, where no stripping was observed. Above 500 mV, the coverage dropped quickly to a plateau near 3/4 ML, and then slowly rolled off again at still higher potentials. The final method involved cathodically stripping of excess Se. Again, the first step involved deposition of 1.25 ML of Se. However, in this method, the solution was next

exchanged for a blank, with no Se containing species, and the electrode was poised at relatively negative potentials to reduce excess Se to Se^{2-}. Figure 5 shows the Se coverages left after cathodic stripping in three different blank solutions: pH 2, pH 4, and pH 9. In each case, the coverage dropped to near 1/2 ML at the most negative potentials studied. In general, the Se was found to strip rapidly, normaly taking less then 10 seconds to strip. It proved very difficult, however, to remove the last 1/2 ML of Se by reduction. In the case of the highest pH solution, pH 9, an intermediate plateau was observed for about 3/4 of a monolayer, reminiscent of the central plateau in Figure 4. This last method has increased importance in this group, as it corresponds to the conditions presently used to form Se atomic layers during an ECALE cycle. Formation of Se atomic layers, after formation of a Cd or Zn atomic layer, by either of the other two methods (cathodic deposition or anodic stripping) also resulted in removal of the previously deposited Cd, or Zn, in cycles for the formation of CdSe, or ZnSe, respectively.

Se Atomic Layer Structures

To investigate structures formed during the deposition of atomic layers of Se, studies were performed using STM and UHV-EC techniques. STM imaging was performed both in air and *in situ*. Most of the studies described below were performed by first forming deposits under a given set of condition, such as discussed above, and then imaging the resulting deposit. In the UHV-EC studies, low energy electron diffraction (LEED) and Auger electron spectroscopy (AES) were used to study the deposits. Well ordered Se deposits were identified using LEED, and AES was used to determine surface cleanliness. Quantification of deposited Se by Auger, however, was not performed as the Auger yield proved too low.

The LEED pattern observed at the lowest Se coverages, 1/4 ML (determined electrochemically), was a p(2X2) (Figure 6A) [41]. There was no evidence for the formation of a distinct 1/4 coverage p(2X2) structure in the voltammetry shown in Figure 2, however. The structure was formed by holding the potential at a point half way down the first UPD peak, or by stripping a bulk deposit of Se at 675 mV. This p(2X2) structure was anticipated from previous studies of Te atomic layer formation on Au(100) [12,13], where a prominent 1/4 coverage p(2X2) was also formed. Figure 7 displays a fairly noisy STM image of the p(2X2)-Se structure, formed as described above. In the STM images, the [110] direction, along the rows of Au atoms in the Au(100) substrate, is oriented at 45° to the image horizontal. This p(2X2) structure was not easy to image for two reasons: first, it was difficult to find conditions where the 1/4 coverage structure would form homogeneously over the surface, as a number of higher coverage Se structures were also stable at similar potentials. Second, it was hard to image the Se atoms at such a low coverage, due to the absence of close packing in the Se layer. This loose packing is evident in Figure 6A, where the Se atoms have been drawn at their van der Waals diameters, 0.40 nm.

A second ordered LEED pattern, a $(2X\sqrt{10})$, was observed when the deposition was carried out to the peak of B (Figure 2) and then emersed (removed from solution), or by depositing at 357 mV for 5 minutes (Figure 3). The $(2X\sqrt{10})$ was, again, familiar from previous studies of Te atomic layer formation [12,13]. The $(2X\sqrt{10})$ structure is easily recongnized from STM (Figure 8) by the characteristic zig-zag chains of chalcogenide atoms. A structure consistent with the LEED, STM and coulometry, is shown in Figure 6B, and has the Se atoms at a coverage of 1/3, and set in four fold sites. The Se-Se distance between atoms in the chains is ✓2 times the Au-Au distance (about 0.4 nm, very close to the van der Waals distance). Figure 8 was obtained *in-situ* in a 1 mM H_2SO_4 solution, after deposition of 1/3 ML of Se from a 1 mM

$HSeO_3^-$ solution at 357 mV. The solution was exchanged, from $HSeO_3^-$ to H_2SO_4, in order to prevent deposition of Se on the W tip while imaging, as the tip had to be kept at a negative potential, while *in situ*, to prevent its oxidation. The image displays two domains of the (2X✓10)-Se structure, rotated by 90° from each other. Some drift is evident in the image.

Deposition to the valley between peaks B and C in Figure 2, or poising the potential at 305 mV for 5 minutes, resulted in a well ordered c(2X2) LEED pattern. Coulommetry indicated a coverage of near 1/2 ML, as shown in Figure 3. A c(2X2) pattern generally indicates 1/2 ML coverage in the formation of an atomic layer, as the primitive unit cell, $(\sqrt{2}\,X\sqrt{2})R45°$, is comprised of only two Au substrate atoms, so the possible atomic layer coverages are then 1/2 and 1, where a coverage of 1 is generally degenerate with the substrate. Evidently, B in Figure 2 corresponds to conversion of the $(2X\sqrt{10})$-Se structure at 1/3 ML coverage, to the c(2X2)-Se structure at 1/2 ML coverage (Figure 6B-C).

An STM image of a deposit formed under the above conditions is shown in Figure 9, and shows the c(2X2) structure to cover the majority of the surface. There are, however, some other interesting features in Figure 9, including obvious domains of the $(2X\sqrt{10})$ and a number of bright clusters.

Deposits formed with still higher coverages, 0.5-0.7 ML, revealed more and more of the bright clusters (Figure 10). Close examination of the clusters shows them to be square rings. Profiles of the rings in Figure 9 indicates that they rise above the atoms in the c(2X2)-Se structure by only about 0.1 nm. Given this low profile, and the fact that the rings begin to form at coverages as low as a 1/2 ML, it appears that they are formed in the first Se atomic layer, on the Au substrate, and are not part of a second Se layer (Figure 6D). Measurements of the rings indicate a side length of 0.54 nm, significantly longer than 0.4 nm Se-Se distances in the c(2X2) structure. If the rings were composed of four Se atoms, then their formation would involve the

spreading apart of Se atoms from the c(2X2), which is counter intuitive considering the fact that the Se coverage is increasing. The brightness of the rings, compared with the surrounding Se atoms, indicates that the atoms are higher up or that the tunneling probability is higher for Se atoms in the rings, under the tunneling conditions used. Both explanations appear consistent with the Se atoms forming an eight membered ring molecule on the surface. Eight membered rings of chalcogenides are well known. Both S and Se occur naturally as eight membered rings [42]. Three of the allotropes of Se consist of eight membered rings. The naturally occurring 8-membered rings of Se and S, however, are not square but puckered, with Se-Se-Se angles of near 105°. Constraint of a chalcogenide ring to the planar-square configuration is energetically unfavorable. However, given the presence of eight Se-Au bonds, the square configuration is reasonable. Planar S_8 rings on other Au substrates have been observed by several other workers [27,28].

The 1/2 coverage c(2X2) structure appears to be the conversion point. That is, any addition of Se above 1/2 coverage resulted in the formation of the Se_8 rings on the surface. It is probable that noise observed in Figure 9 represents precursors to the formation of the rings. The noise does not appear in the $(2X\sqrt{10})$ domains, where the Se density is lower, but only in the c(2X2) domains. The light streaks, noise, could easily be places where two or three Se atoms are bound together. The fact that the two and three atom clusters appear as streaks is an indication that they are either very mobile or fragile, unstable to the tunneling conditions until a ring is complete.

For deposits formed with coverages above 1/2, the c(2X2) LEED pattern began to fade, converting to a number of diffuse streaks. At coverages above 3/4, the c(2X2) spots were gone, and the "box" LEED pattern shown in Figure 11 was observed. These conditions were easily produced by scanning partially into peak C (Figure 2), until coulometry indicated that the desired

coverage was obtained. Additionally, the box pattern was observed under conditions corresponding to the plateaus in Se coverage near 3/4 ML, obtained after anodic (Figure 4) or cathodic (Figure 5) stripping.

STM images taken under the above conditions, revealed the structure shown in Figure 12, which appears to consist of close packed Se_8 rings. Not all the rings are missing an atom in the center, some areas look more like a close packed layer of Se atoms. The extent to which the centers of the rings are filled appears to be a function of the conditions under which the structure was formed. It might be expected that the rings should form a (3X3) structure if they were packed carefully on the Au(100) surface. Some of the images display a more ordered array of rings than others, but a clear (3X3) was never observed. A two dimensional fast Fourier transform (2D FFT) was performed on the image in Figure 12, and is shown in Figure 13. Clearly displayed in Figure 13 is the same box pattern observed in the LEED pattern, Figure 11. Characteristic bands of intensity perpendicular to the integral beam vectors, at 1/3 and 2/3 of the distance between the specular and the integral beams, are evident and strongly suggest a 3X periodicity in the surface structure, relative to the substrate. Examination of the STM images (Figure 12) shows that many adjacent Se_8 rings are shifted by one Au-Au distance between rows of rings. This shift of up three and over one results in a $\sqrt{10}$ distance. Figure 14 is a calculated LEED pattern for a $(3X\sqrt{10})$ unit cell [43], which shows lines of five fractional order beams at the 1/3 and 2/3 distances, where the diffuse bars are observed in both the LEED pattern and the 2D FFT pattern. Figure 15 is a drawing of a proposed $(3X\sqrt{10})$ structure, consistent with the above data.

A comparison of the Se_8 rings formed as isolated features (Figures 6D and 10), with the closed packed structure (Figure 12), reveals a 45° rotation of the rings. Close inspection of Figure 10 shows that some domains of the rotated close packed rings are present along with the more

isolated rings. There are clear indications that these rings are molecules, and mobile on the surface. That is, under some tunneling conditions, the rings appear to move across the surface from scan to scan. The close packed layers probably nucleate at some step site, and then grow as rings diffuse across the surface, rotate, and pack into the ($3X\sqrt{10}$) lattice.

Another feature of the Se_8 ring structures is that as they form, a series of pits are formed on the surface as well. Figure 16 is of a surface covered with the close packed Se rings. The pits are clearly evident. Height measurements made on this surface show the pits to be one Au atomic layer deep. The pit bottoms were easily imaged, as well, and showed the same close packed Se rings. Two pits are clearly visible in Figure 10, where the ($3X\sqrt{10}$) structure has just begun to form.

The pits in Figures 10 and 16 are reminiscent of the pits observed in the self assembly of long chain alkanethiols on Au surfaces, which have been studied extensively using techniques sensitive to surface morphology, such as STM [29-35] and atomic force microscopy (AFM) [44]. There are presently several proposed origins for the pits, including: defect sites [29,30], Au etching [32-35], alloy formation, and shrinking of the Au surface atoms [31]. With regard to the present studies, the same structures exist inside the pits as on the surface, indicating that defect sites or contamination are probably not the primary cause of their formation. A quartz crystal microbalance study of pit formation on Au in a Na_2S solution indicated that a sufficient mass loss was recorded to account for the pits [45]. Alloy formation is another possibility. In STM studies of the alloying of Pb with Au, however, pits were observed to form as the Pb was stripped from the surface, not after deposition [46]. In the present studies, the pits were observed to go away as the Se coverage was decreased below 1/2, suggesting that the lateral extent of the Au atoms on the surface may decrease as the ring structures form. That is, the Se-Se bond

distance in the Se_8 rings of red Se is 0.23 nm, considerably less than the 0.28 nm observed from the STM images. This, together with flattening out the rings to bring all the Se atoms in contact with the Au surface, could result in significant stress between the Se and Au, and thus compression of the Au surface atoms.

The pits are not large, generally around 3 nm, and are evenly distributed over the surface. This suggests that the phenomenon that is causing them is, initially, homogeneously distributed. The fractional surface area comprising the pits is about 11%, on the average. If the diameter of the Au atoms were to decrease from 0.292 to 0.275 nm, the pits could be accounted for. The calibration of the STM is not perfect, and there is generally some drift in the images, but by using comparisons with known structures like the ($2X\sqrt{10}$), the dimensions of the Se_8 molecules in the ring structures were determined and appear to have dimensions close to those that could account for the pit formation.

CONCLUSIONS

A sequence of well ordered atomic layers of Se were formed electrochemically on Au(100). Three different electrochemical methods were used to form the atomic layers: direct reduction from a selenite solution; initial deposition of 1.25 ML of Se, followed by oxidative stripping; and initial deposition of 1.25 ML of Se, followed by reductive stripping. The Se structures observed included: a 1/4 coverage p(2X2), followed by a 1/3 coverage ($2X\sqrt{10}$), and then a 1/2 coverage c(2X2). At coverages exceeding 1/2, Se_8 rings began to form on the surface. As the coverage increased to near 3/4 ML, the rings began to undergo an apparent 45° rotation and close packed, forming a mainly ($3X\sqrt{10}$) structure. The Se_8 rings behave like individual molecules on the surface, as they move and pack into the growing structure.

One of the motivations for this work was to form a 1/2 coverage Se atomic layer to use as a substrate for subsequent Cd deposition and formation of CdSe by ECALE. A c(2X2) structure, with a 1/2 ML coverage, was formed but not as homogeneously as desired. Most of the other stable Se atomic layer structures were formed to some extent under these conditions, as well. The problem appears to be slow deposition kinetics. That is, all the structures were formed at overpotentials, so that is was very difficult to select conditions were a single thermodynamically stable structure was formed, except for the (3X$\surd$10). The close packed Se_8 ring structure, mainly a (3X$\sqrt{10}$), could be formed homogeniously on the surface, but at coverages greater than 3/4 ML.

The main problem with forming the 1/2 ML c(2X2) structure was the slow kinetics for deposition. That is, the formal potential for the $HSeO_3^-$/Se couple in the studies presented here was close to 400 mV, however, all the structures observed in the present studies were formed at considerably more negative potentials. That is, deposits in the present study were formed at over potentials.

At the higher coverages, structures consisting of Se_8 rings and pits, one Au atomic layer deep, were observed to form. The pits resemble features seen on . Au surfaces where self assembled monolayers of alkane thiols, SAMs, have been formed. The pits disappear when the Se_8 ring structures, near 3/4 ML coverage, were anodically stripped, forming a 1/4 coverage p(2X2) structure. Although there have been a number of explanations put forward for the pit formation, the two most probable are that some etching of the Au surface is taking place along with reduction selenite solution, or that there is a decrease in the lateral extent of the Au surface atoms, due to mis-match stress between the rings and the Au surface atoms.

ACKNOWLEDGMENT

This work was supported in part by the Navy, Office of the Chief of Naval Research (ONR), under grant #N00014-91-J-1919, and by the National Science Foundation (NSF), under grant #DMR-9017431. This financial assistance is gratefully acknowledged.

REFERENCES

1) Suntula, T.; Anson, J. *U. S. Patent* 4,058,430 (1977).

2) *Atomic Layer Growth and Processing*; MRS Symp. Proc., Vol. 222, Eds. T.F. Kuech, P.D. Dapkus, Y. Aoyagi, (MRS, Pittsburgh, 1991).

3) *Atomic Layer Epitaxy*; Ed. S. Bedair, (Elsevier, Amsterdam, 1993).

4) J.L. Stickney, B.W. Gregory, I. Villegas, *U.S. Patent* 5,320,736 (1994).

5) B.W. Gregory, J.L. Stickney, *J. Electroanal. Chem.* 300 (1991) 543.

6) B.W. Gregory, D.W. Suggs, J.L. Stickney, *J. Electroanal. Chem. 138* **(1991)** 1279.

7) D.W. Suggs, I. Villegas, B.W. Gregory, J.L. Stickney, in *Atomic Layer Growth and Processing*; MRS Symp. Proc., Vol 222, Eds. T.F. Kuech, P.D. Dapkus, Y. Aoyagi, (MRS, Pittsburgh, 1991) pp 283.

8) B.M. Huang, T.E. Lister, J.L. Stickney, In *CRC Handbook of Surface Imaging and Visualization, Ed.* A.T. Hubbard (CRC Press: Boca Raton, 1995) pp. 75.

9) D.M. Kolb, in *Advances in Electrochemistry and Electrochemical Engineering*; Vol. 11, Eds. H. Gerischer, C.W. Tobias, (Wiley, New York, 1978) pp. 125.

10) K. Jutter, W.J. Lorenz, *Z. Phys. Chem. N. F.* **122 (1980)** 163.

11) R.R. Adzic, in *Advances in Electrochemistry and Electrochemical Engineering, Vol. 13,* Eds. H. Gerischer, C.W. Tobias, (Wiley-Interscience, New York, 1978) pp 159.

12) D.W. Suggs, J.L. Stickney, *J. Phys. Chem.* 95 (1991) 10056.

13) D.W. Suggs, J.L. Stickney, *Surf. Sci.* 290 (1993) 362, 375.

14) I. Villegas, J.L. Stickney, *J. Electrochem. Soc.*, 139 (1992) 686.

15) I. Villegas, J.L. Stickney, *J. Vac. Sci. Technol.* **A,** 10 (1992) 3032.

16) B.W. Gregory, D.W. Suggs, J.L. Stickney, *J. Electrochem. Soc.* 138 (1991) 1279.

17) B.W. Gregory, M.L. Norton, J.L. Stickney, *J. Electroanal. Chem., 293* (1990) 85.

18) B.M. Huang, L.P. Colletti, B.W. Gregory, J.L. Anderson, J.L. Stickney, *J. Electrochem. Soc.*, 142 (1995) 3007.

19) C.K. Rhee, B.M. Huang, E.M. Wilmer, S. Thomas, J.L. Stickney, *Materials and Manufacturing Processes*, 10 (1995) 283.

20) C. Wei, N. Myung, K. Rajeshwar, *J. Electroanal. Chem., 275 (***1994)** 109.

21) R.W. Andrews, D.C. Johnson, *Anal. Chem.* 47 (1975) 294.

22) M.K. Kazacos, B. Miller, *J. Electrochem. Soc.* 127 (1980) 869.

23) R. Czajka, A. Kasuya, N. Horiguchi, Y. Nishina, *J. Vac. Sci. Technol.* B. 12 (1994) 1890.

24) D.W. Suggs, J.L. Stickney, *J. Phys. Chem.* 95 (1991) 10056.

25) D.F. Ogletree, C. Ocal, B. Marchon, G.A. Somorjai, M. Salmeron, T. Beebe, W.J. Siekhaus, *J. Vac. Sci. Technol.* A, 8 (1990) 297.

26) R.Q. Hwang, D.M. Zeglinski, A.L. Vazquez-de-Parga, D.F. Ogletree, C. Ocal, G.A. Somorjai, M. Salmeron, D.R. Denley, *Phys. Rev. B, 44* **(1991)** 1914.

27) X. Gao, Y. Zhang, Y., M.J. Weaver, *J. Phys. Chem.* 96 (1992) 4156.

28) R.L. McCarley, Y.-T Kim, A.J. Bard, *J. Phys. Chem.* 97 (1993) 211.

29) Y.-T. Kim, A.J. Bard, *Langmuir*, 8 (1992) 1096.

30) T. Han, T.P. Beebe, Jr., *Langmuir* , 10 (1994) 2705.

31) O. Chailapakul, L. Sun, C. Xu, R.M. Crooks, *J. Am. Chem. Soc.* 115 (1993) 12459.

32) K. Edinger, A. Golizhauser, K. Demota, Ch. Woll, M. Grunze, *Langmuir* 9 (1993) 4.

(33) C. Schonenberger, J.A.M. Sondag-Huethorst, J. Jorritsma, L.G.J. Fokkink, *Langmuir* 10 (1994) 611.

(34) G.E. Poirier, M.J. Tarlov, *Langmuir* 9 (1994) 2853.

35) G.E. Poirier, M.J. Tarlov, H.E. Rushmeier, *Langmuir*, 10 (1994) 3383.

36) L. Goetting, B.M. Huang, T.E. Lister, J.L. Stickney, *Electrochimica Acta* **40 (1995)** 143.

37) J.F. Rodriguez, T. Mebrahtu, M.P. Soriaga, *J. Electroanal. Chem. 233* **(1987)** 283.

38) H. Siegenthaler, K. Juttner, E. Schmidt, W.J. Lorenz, *Electrochimica Acta*, 23 (1978) 1009.

39) J.L. Stickney, S.D. Rosasco, D. Song, M.P. Soriaga, A.T. Hubbard, *Surface Sci.*, 130 (1983) 326.

40) R.D. Herrick, II, J.L. Stickney, in *New Directions in Electroanalytical Chemistry*, ACS Symp. Proc., Eds. J. Leddy, (ACS, Washington,) submitted.

41) T.E. Lister, B.M. Huang, R.D. Herrick II, J.L. Stickney, J. Vac. Sci. Technol. B, 13 (1995) 1268.

42) N.N. Greenwood, A. Earnshaw, *Chemistry of Elements,* (Pergamon Press, Oxford, 1984) pp. 772 and pp. 887.

43) B. Schardt, R. Thiehsen, *Handbook of Calculated LEED Patterns*, unpublished.

44) C.A. Alves, E.L. Smith, M.D. Porter, *J. Am. Chem. Soc.*, 114 **(1992)** 1222.

45) R.L. McCarley, Y.T. Kim, A.J. Bard, *J. Phys. Chem.*, 1993 97, 211.

46) M.P. Green, K.J. Hanson, D.A. Sherson, X. Xing, M. Richter, P.N. Ross, R. Carr, I. Lindau, *J. Phys. Chem.* 93 (1989) 2181.

FIGURE CAPTIONS

Figure 1 Cyclic voltammogram of the clean six-sided Au(100) in 20 mM H_2SO_4 solution. Scan rate: 5mV/sec.

Figure 2 Window opening cyclic voltammetry of the six-sided Au(100) electrode in 1 mM $HSeO_3^-$ and 20 mM H_2SO_4 solution (pH 2). Scan rate: 5 mV/sec. Solid and dashed lines are alternated.

Figure 3 Graphs of the dependence of coverage on the deposition potentials and time. Each point was obtained by scanning to the indicated potential and holding for the indicated period of time. Anodic stripping, following deposition, was used to determine the coverage. Scan rate: 5 mV/sec.

Figure 4 Formation of atomic layer Se by anodic stripping. Each point was determined by first depositing 1 1/4 ML of Se. The deposit was then shifted to the potential indicated and held for 5 minutes. The remaining Se was then determined by oxidative stripping coulometry.

Figure 5 Formation of atomic layer Se by cathodic stripping. Each point was determined by first depositing 1 1/4 ML of Se. The solution was exchanged for one containing no H_2SeO_3, and the potential was shifted to the potential indicated. The deposit was then A) Stripping in 20 mM H_2SO_4, pH 2; B. Stripping in 20 mM NaAc/HAc buffer, pH 4; C. Stripping in 20 mM borate buffer, pH 9.

Figure 6 Diagram of proposed structures for the:

A) p(2X2), 1/4 coverage

B) (2X$\surd$10), 1/3 coverage

C) c(2X2), 1/2 coverage

D) c(2X2) surrounding a Se_8 ring.

Figure 7 STM images of a Au(100)(2X2)-Se, 1/4 ML coverage. The rows of Au atoms are oriented at 45° to the image horizontal.

Figure 8 STM image of a Au(100)(2X$\sqrt{10}$)-Se, at 1/3 ML coverage, obtained *in situ*.

Figure 9 STM image of the Au(100)c(2X2)-Se, at 1/2 ML coverage.

Figure 10 STM image of the clusters formed at over 1/2 ML coverage.

Figure 11 The "box" LEED pattern observed at above 3/4 ML coverage.

Figure 12 STM image of the close packed Se_8 rings, over 3/4 ML coverage. Low pass filtered. The image displays variations on the $(3X\sqrt{10})$ unit cell.

Figure 13 Two dimensional fast Fourier transform (2D FFT) of the STM image in Figure 12, of the close packed Se_8 rings. The same box pattern as observed in LEED, Figure 11, is evident here.

Figure 14 Calculated LEED pattern for a $(3X\sqrt{10})$ on an FCC (100) surface [42].

Figure 15 Drawing of a proposed $(3X\sqrt{10})$ structure.

Figure 16 STM image of a surface covered with the close packed Se rings. Pits are clearly evident. Height measurements made on the surface show the pits to be one Au atomic layer deep.

Huang et al
Figure 1

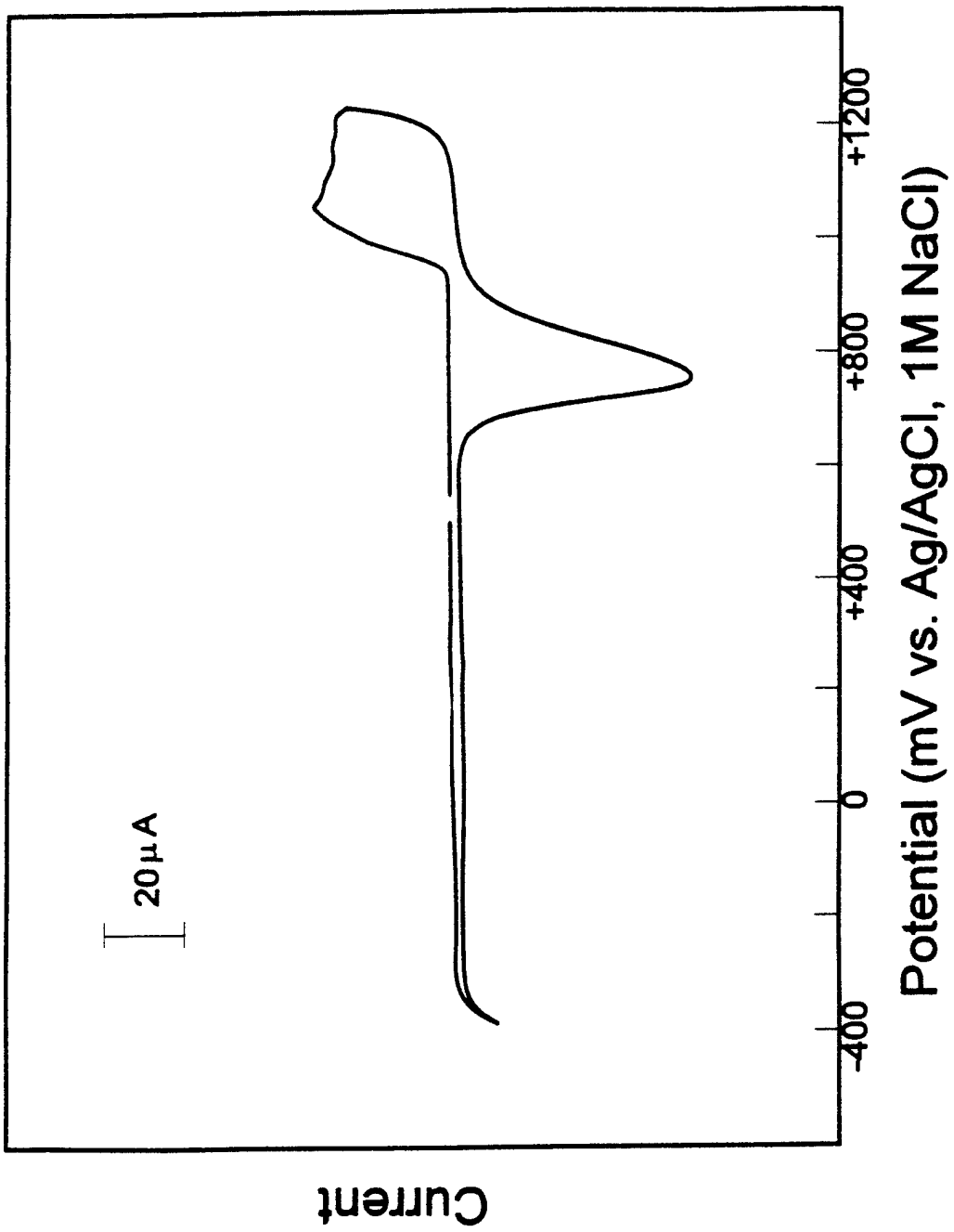

Huang et. al.
Figure 2

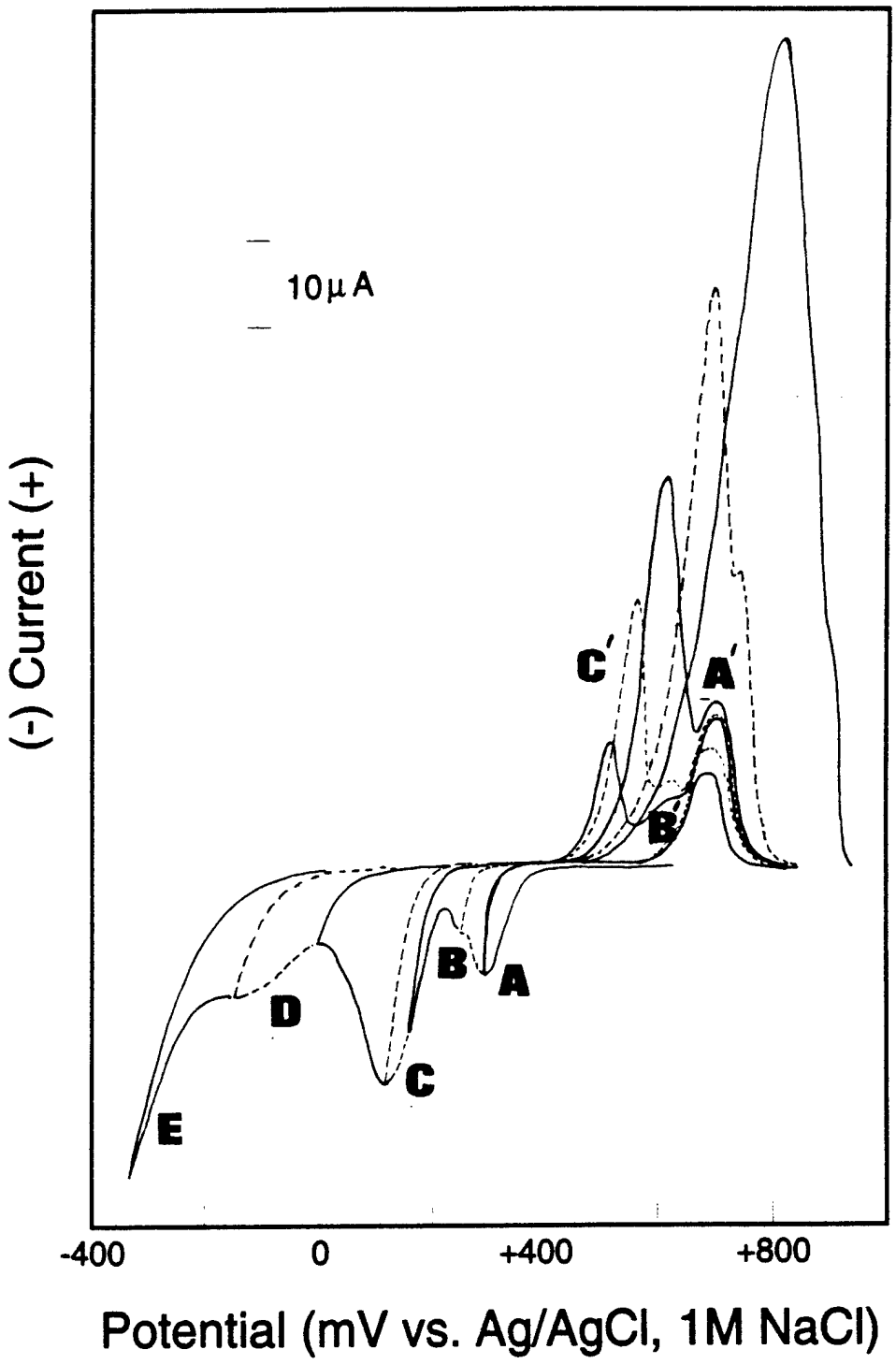

Huang et. al.
Figure 3

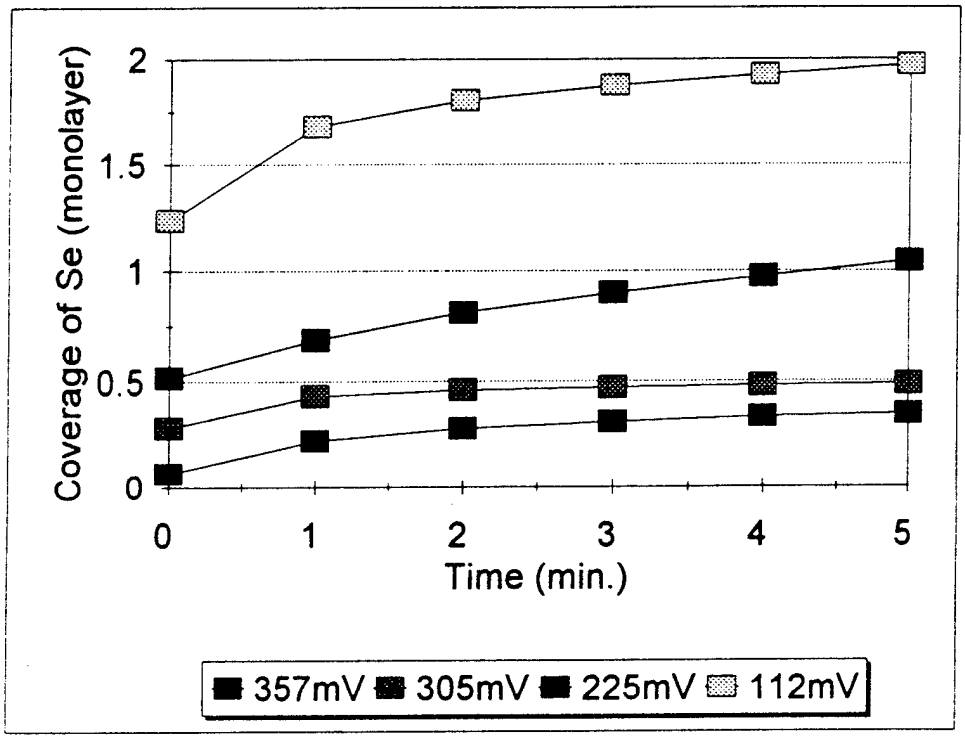

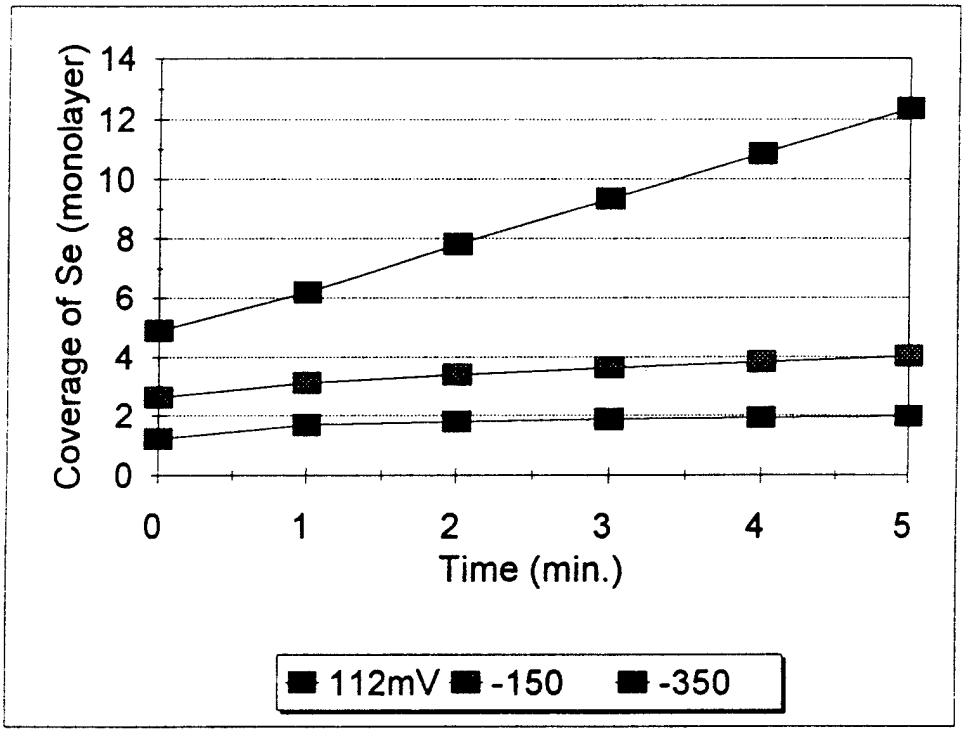

Huang et. al.
Figure 4

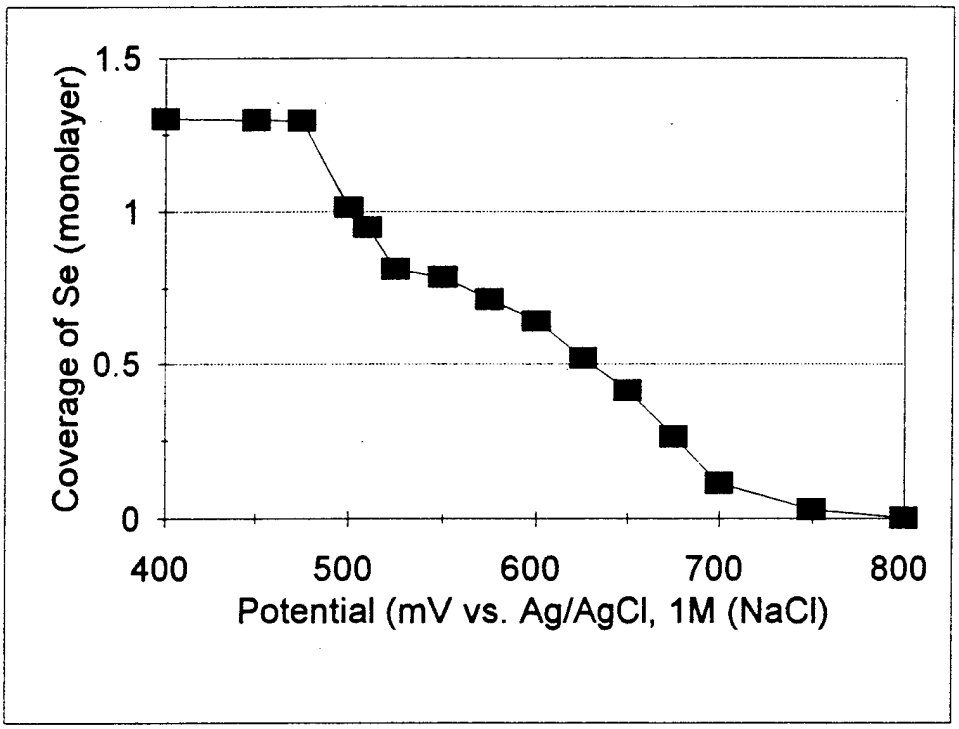

Young et. al.
Figure 5a

A

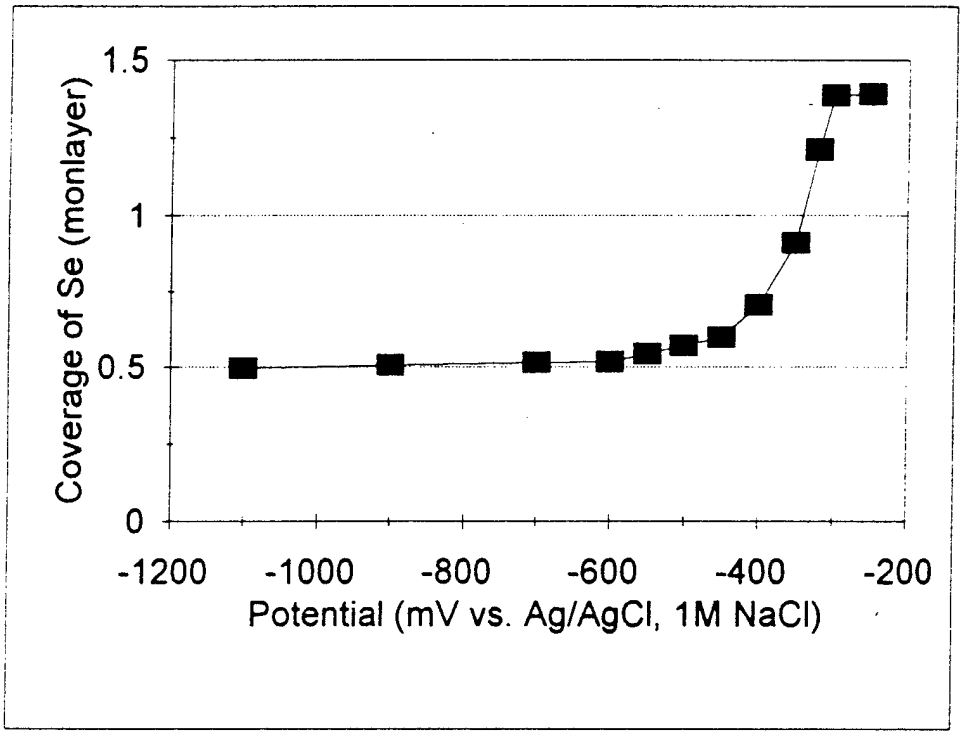

Huang et. al.
Figure 5b

B

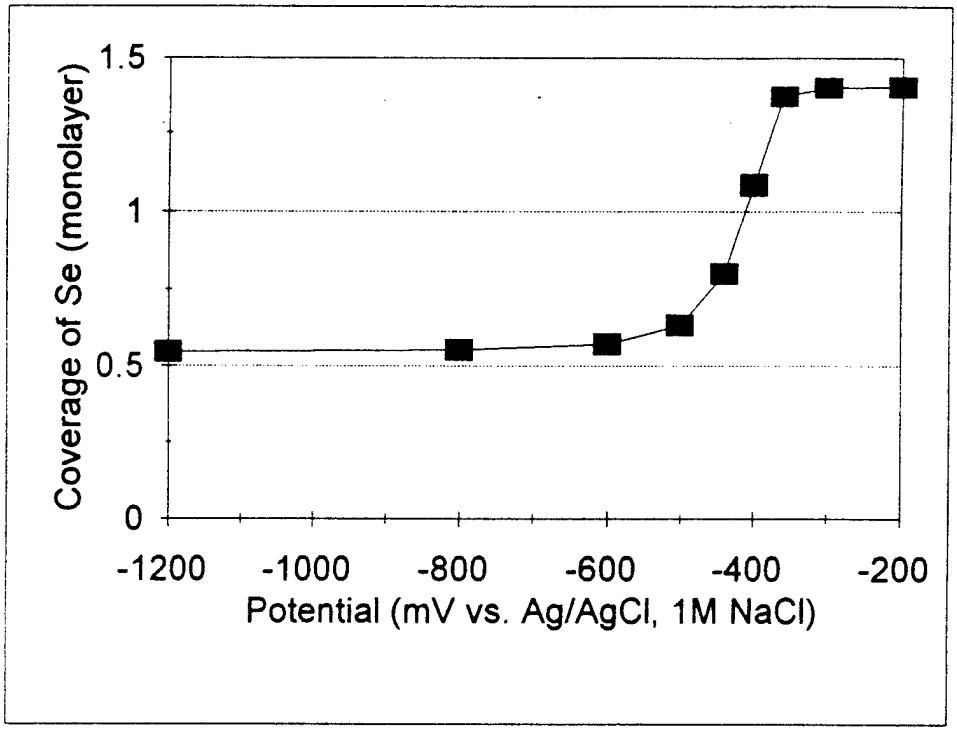

Huang et al.
Figure 5C

C

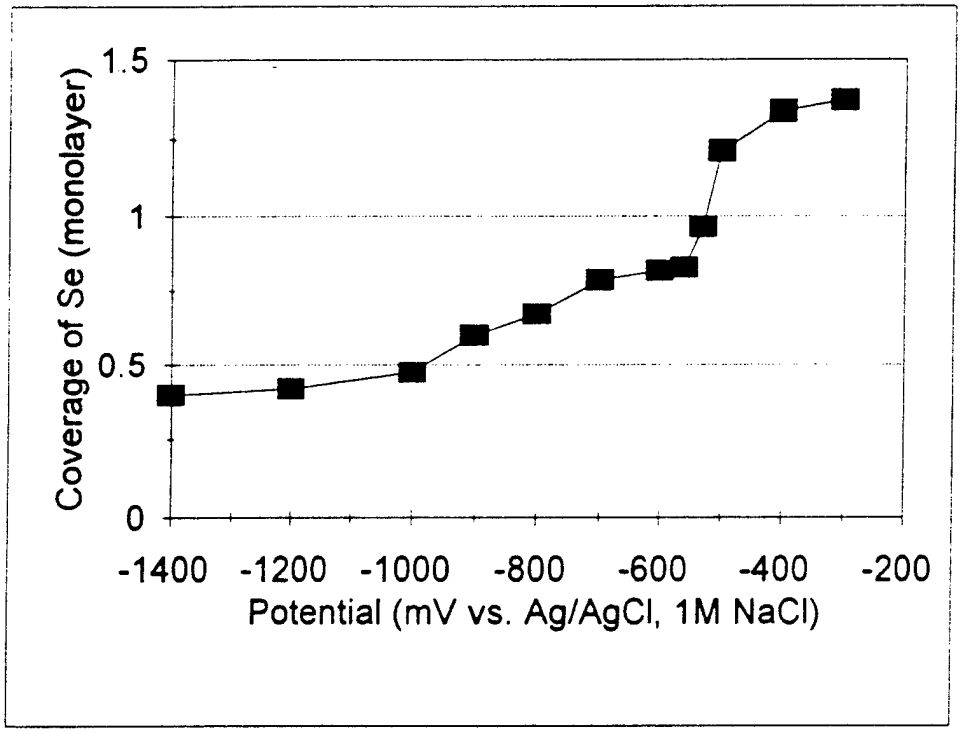

Huang et. al.
Figure 6A

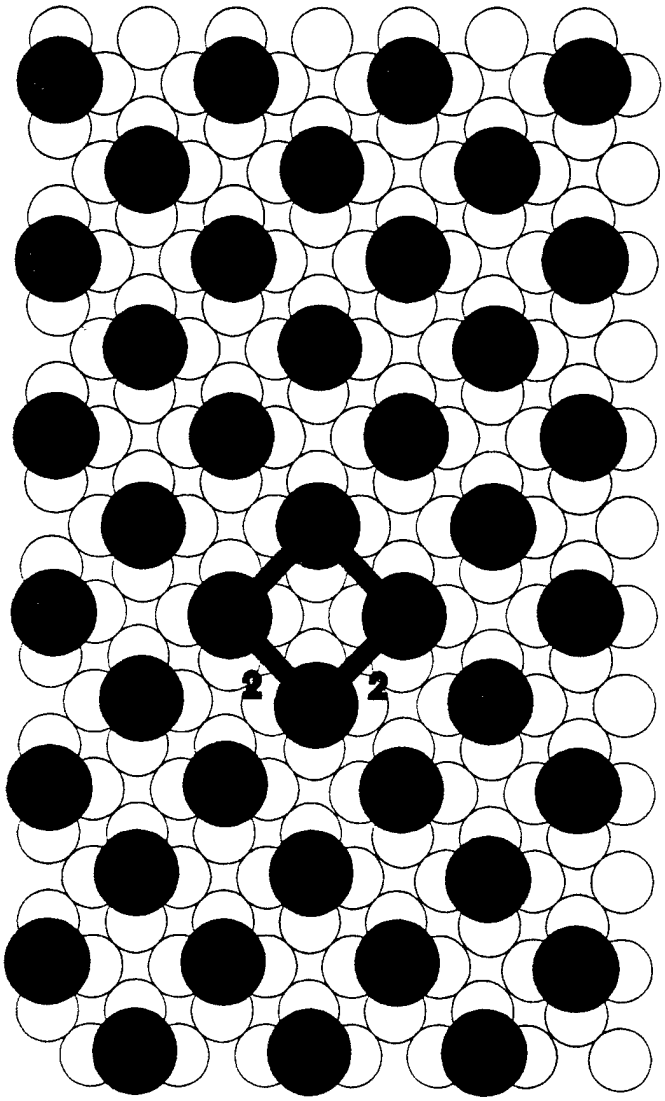

Huang et. al.
Figure 6B

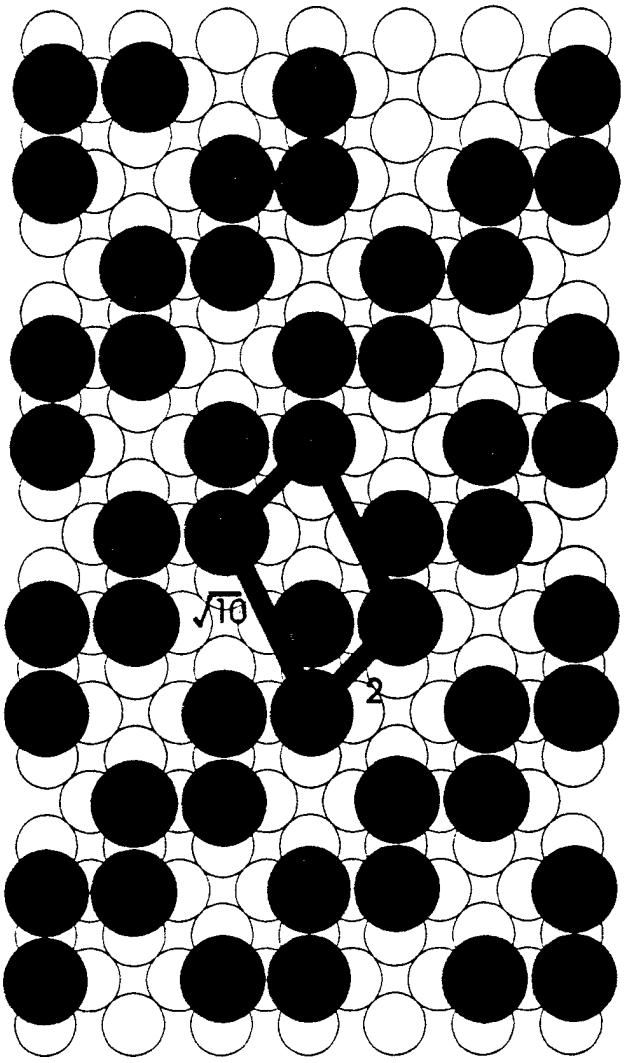

Huang et. al.
Figure 6C

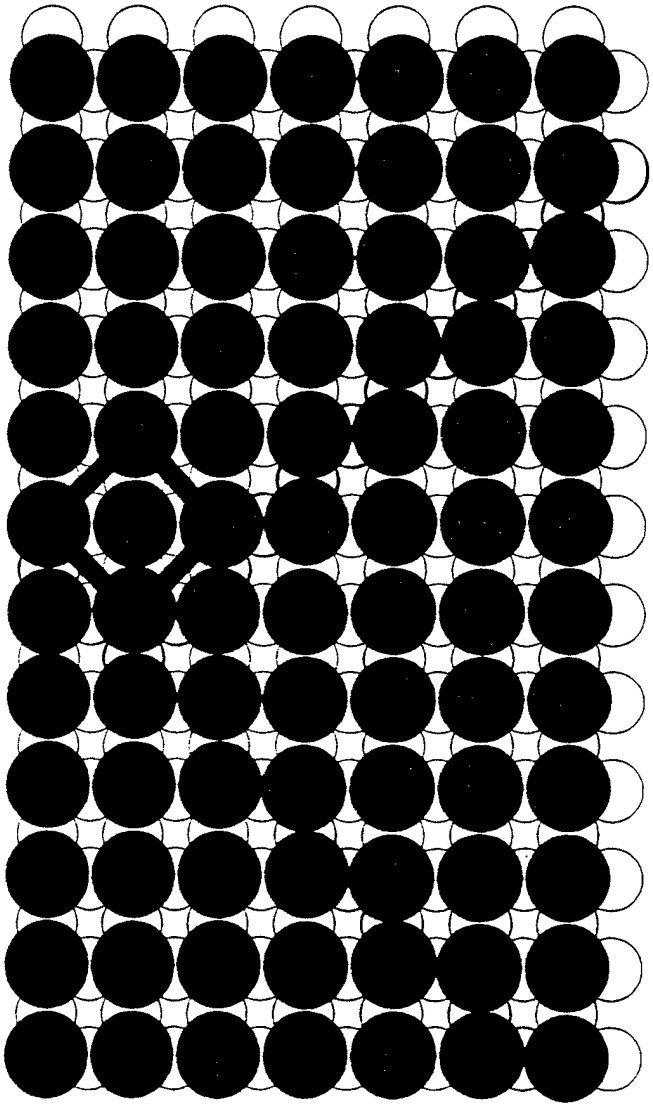

Huang et. al.
Figure 6D

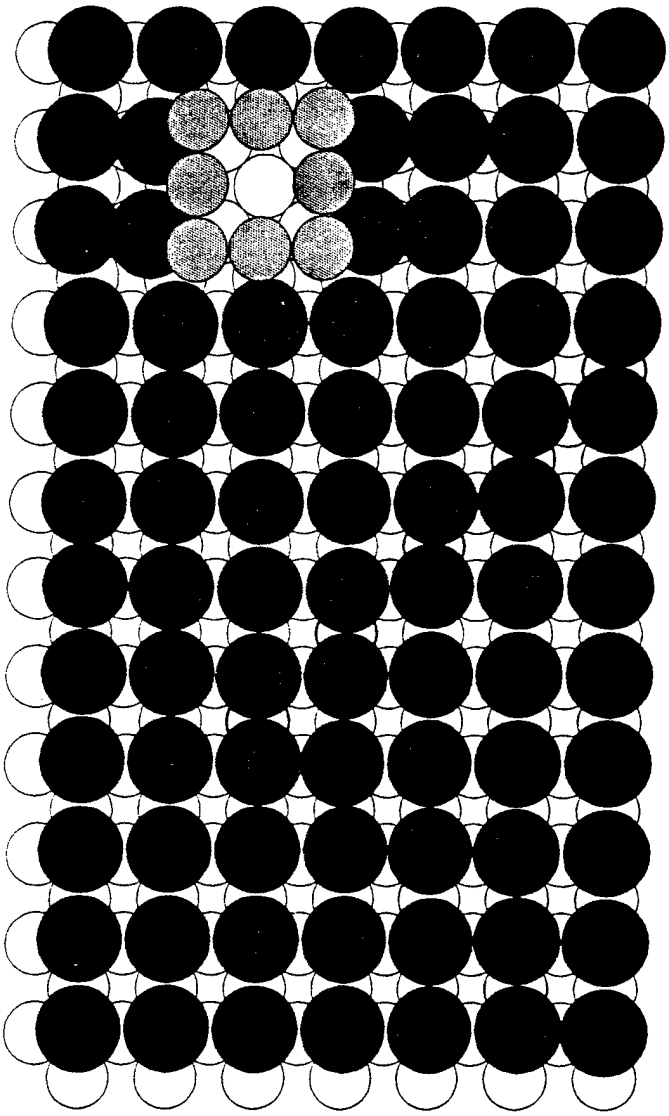

...ng et. al.
Figure #7

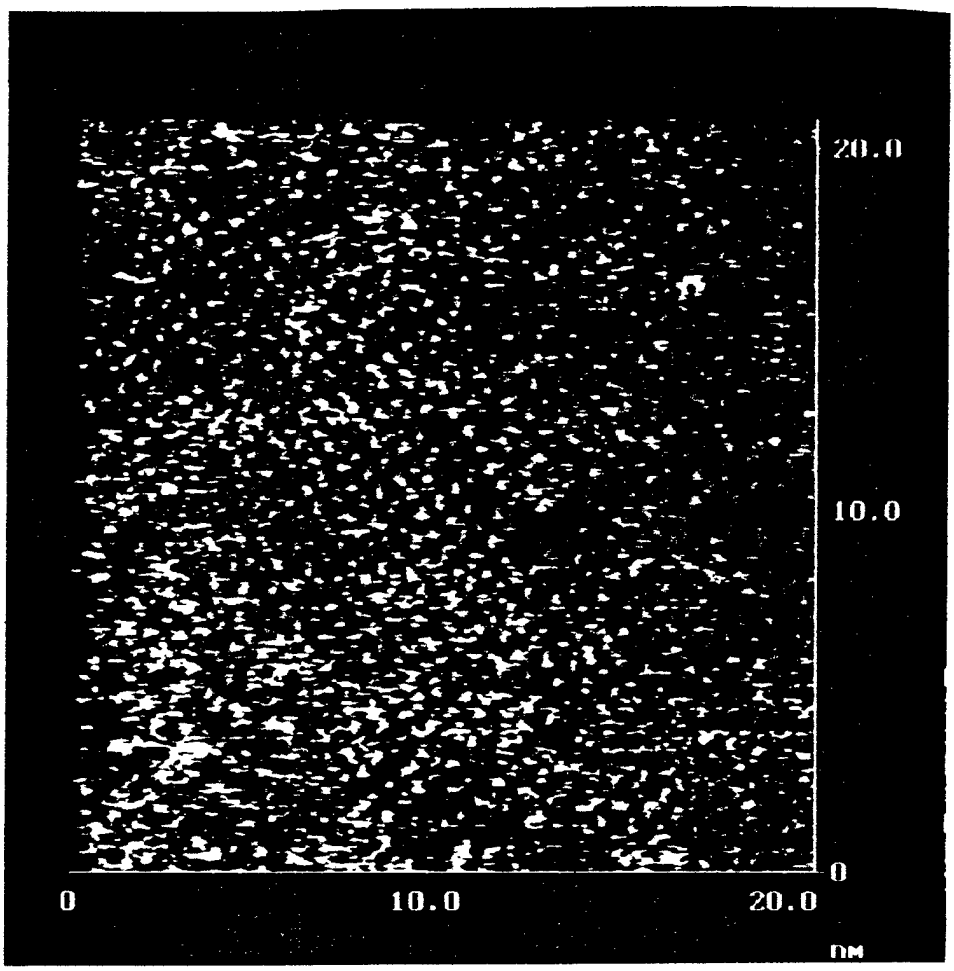

Wang et. al.
Figure 8

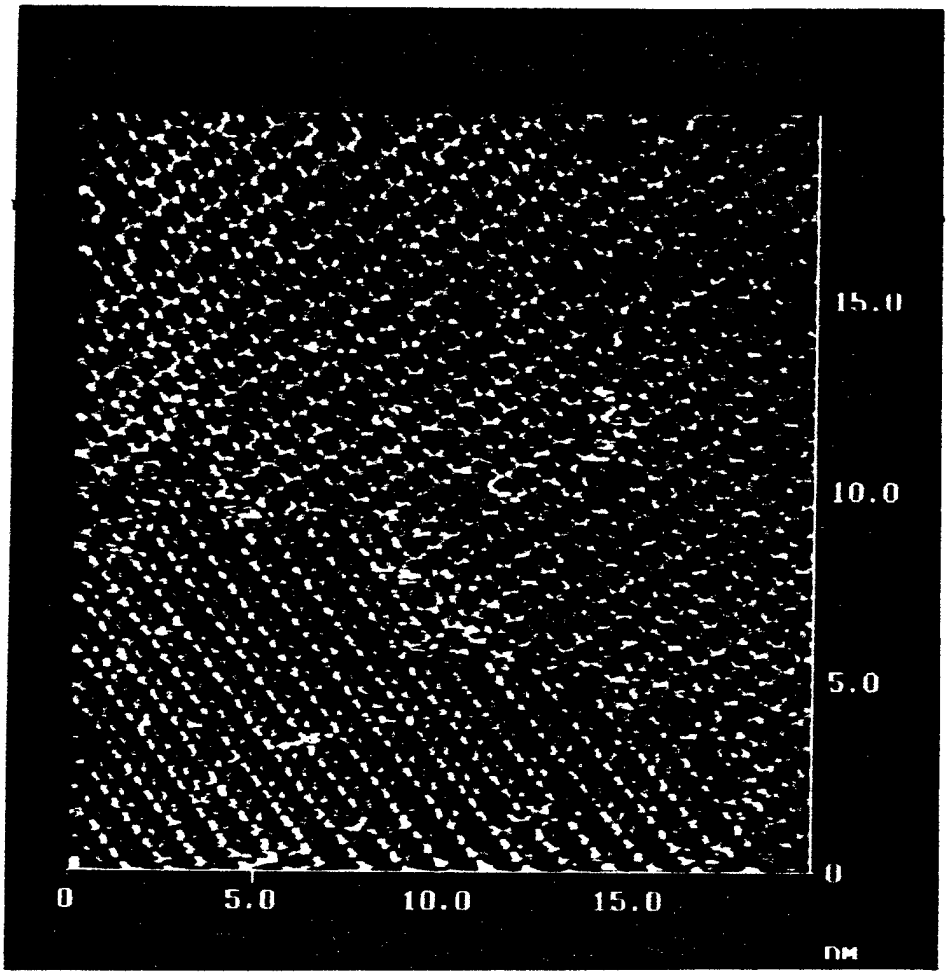

igure 1
Bang et. al.

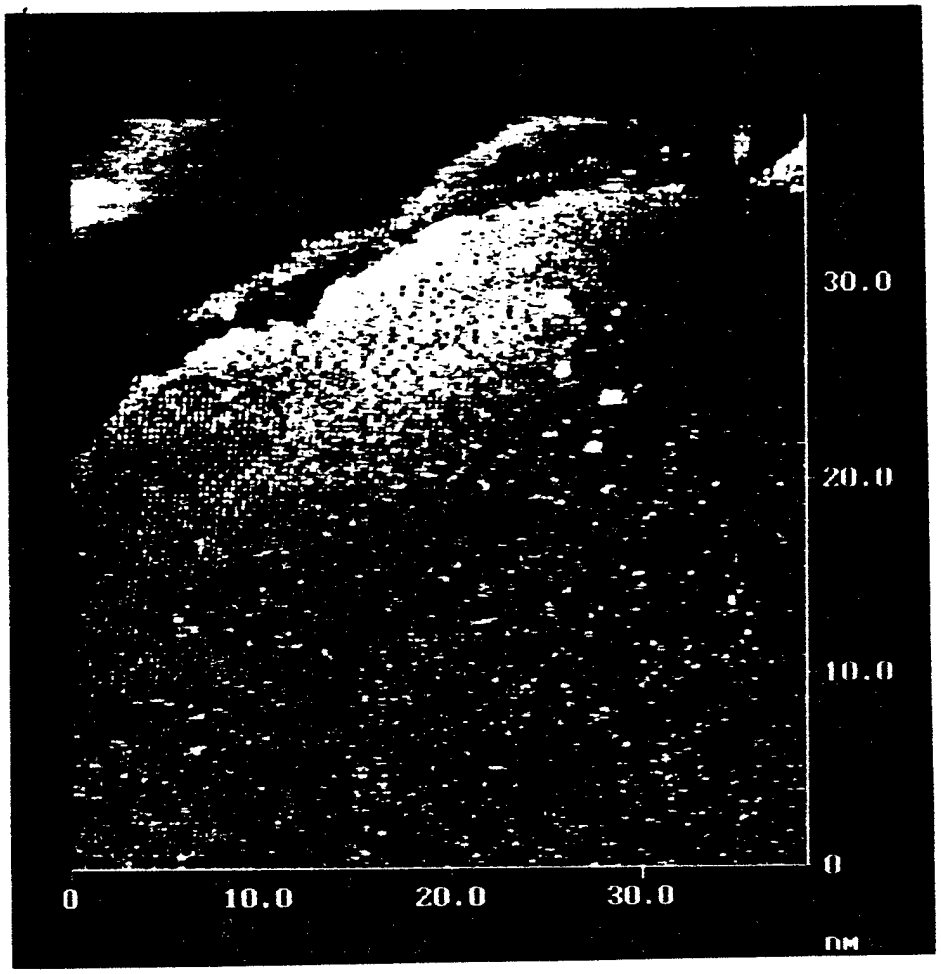

twang et. al.
Figure 10

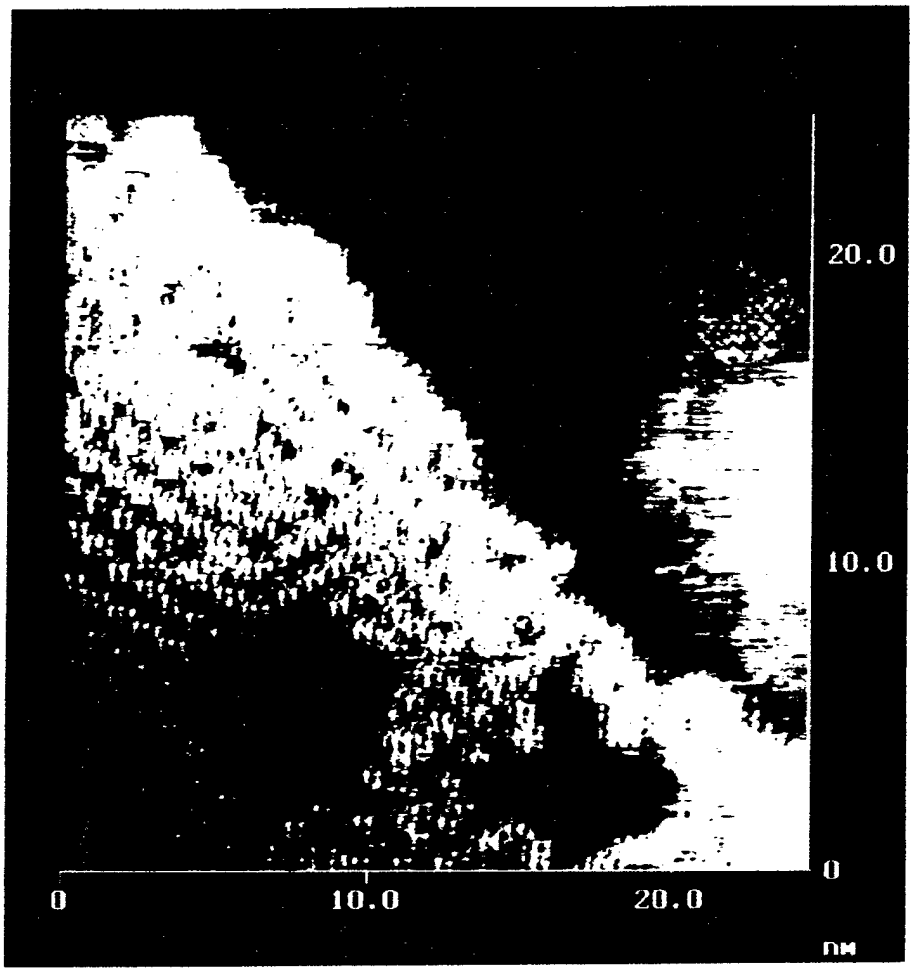

Wang, et. al.
Figure 11

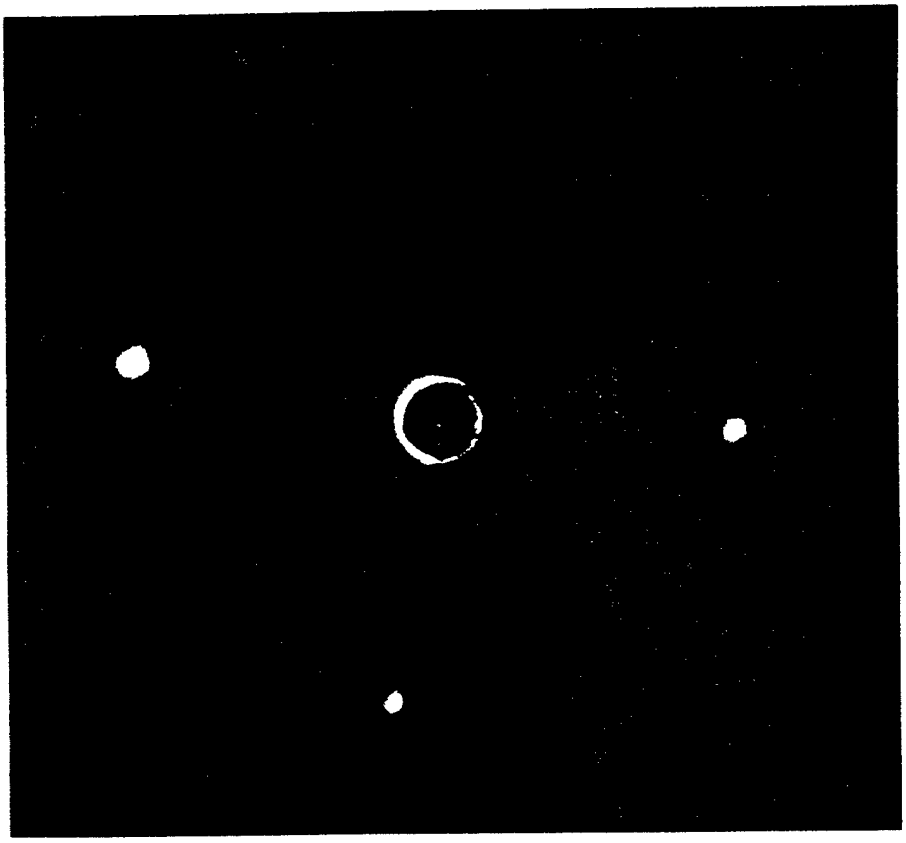

Huang et. al.
Figure 12

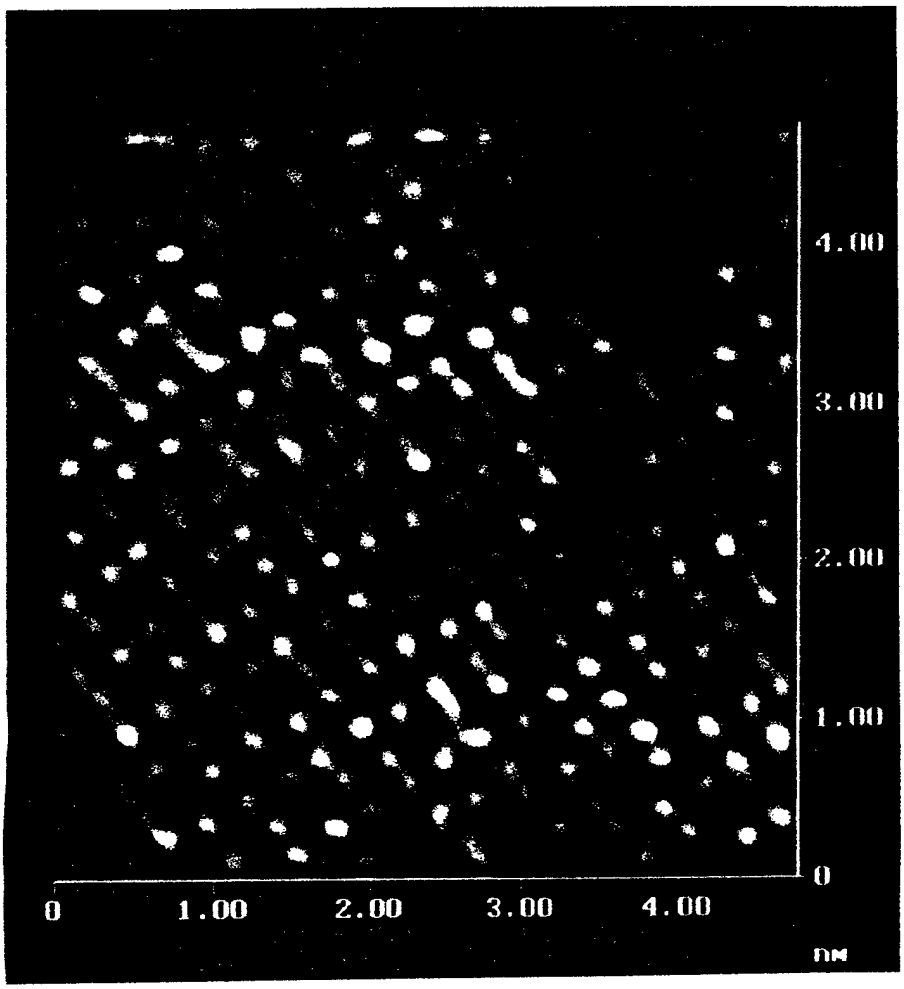

Figure 13
Jiang et al

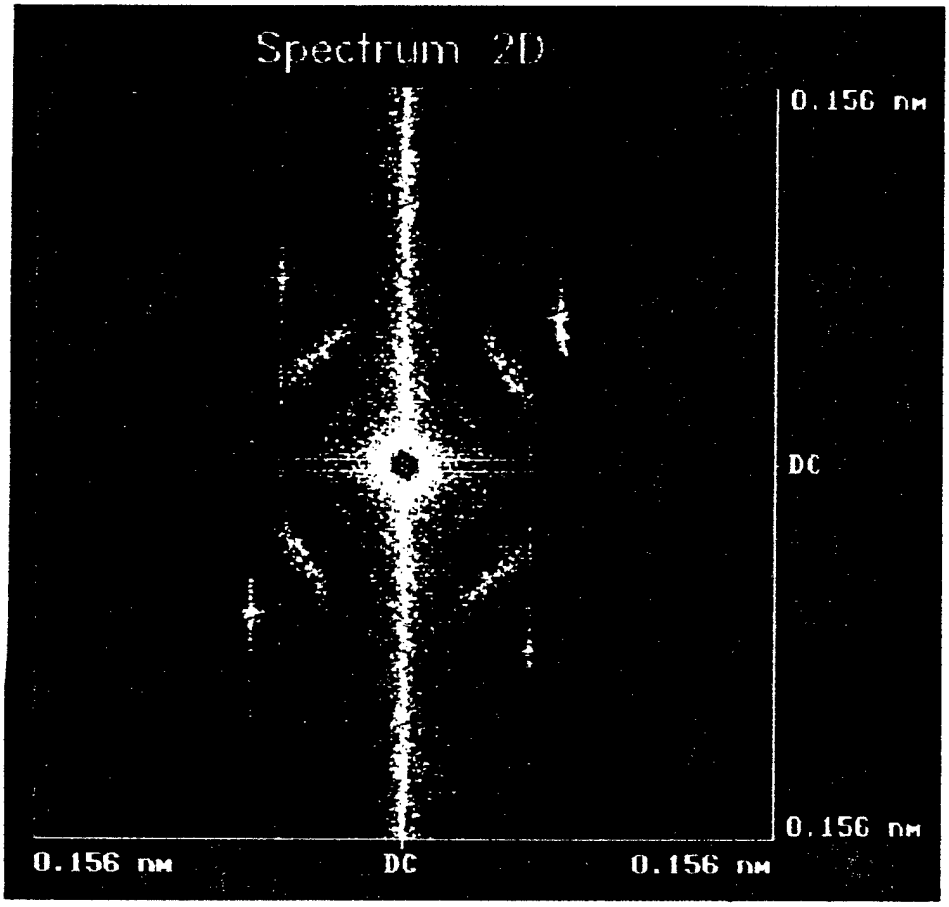

Wang et. al.
Figure 14

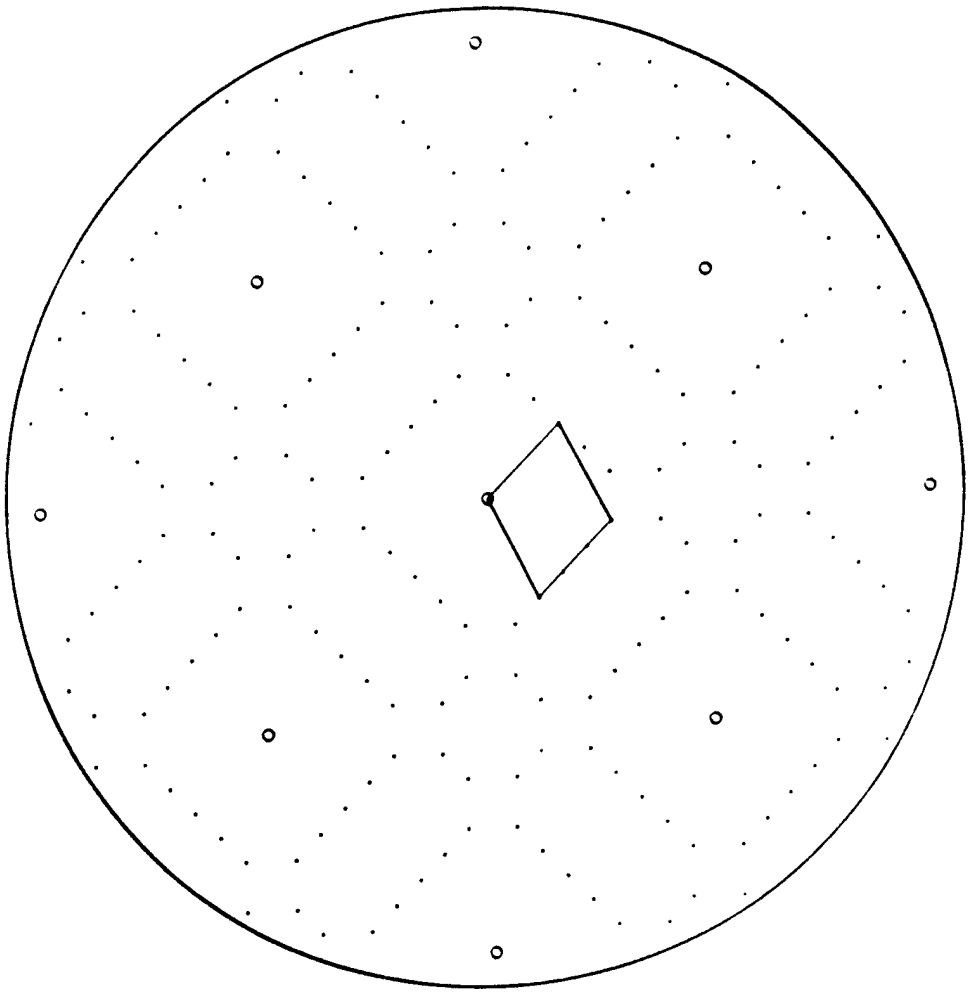

Wang et. al.
Figure #15

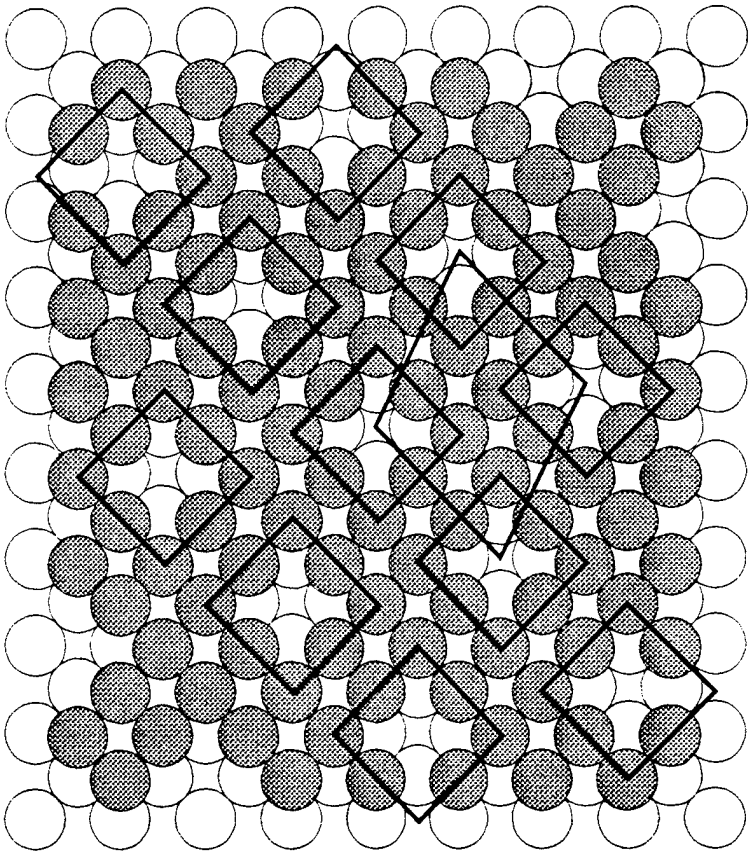

Figure 16
Wang et. al.